

Supporting Information

A new tool to attack biofilms: Driving magnetic iron-oxide nanoparticles to disrupt the matrix

Jie Li, Rachel Nickel, Jiandong Wu, Francis Lin, Johan van Lierop* and Song Liu*

Jie Li¹, Rachel Nickel², Dr. Jiandong Wu², Dr. Francis Lin^{1,2,3}, Dr. Johan van Lierop^{2,3} and Dr. Song Liu^{1,3}

¹ Department of Biosystems Engineering, University of Manitoba, Winnipeg, Manitoba, R3T 2N2, Canada

² Department of Physics and Astronomy, University of Manitoba, Winnipeg, Manitoba, R3T 2N2, Canada

³ Manitoba Institute for Materials, University of Manitoba, Winnipeg, Manitoba, R3T 2N2 Canada

E-mail: Song.Liu@umanitoba.ca; Johan.van.Lierop@umanitoba.ca

Supplementary Figure S1. Transmission Mössbauer spectra of the a) 8, b) 11 and c) 70 nm Fe₃O₄ nanoparticles. The solid lines are fits described in the text.

Supplementary Figure S2. Overlaid size distributions of the 8 (red, dashed line with square caps) and 11 nm (black, dashed line with flat caps) MNPs.

Supplementary Figure S3. (a-b) The ESEM images and (c-d) the SEM images of a control MRSA biofilm.

Supplementary Figure S4. Graph of quantified results of anti-biofilm test for 11 nm MNPs: bacterial numbers of remaining biofilm, treatment and washing solutions and the total bacteria number include bacteria in the remaining biofilm, in the treatment and washing solutions.

Supplementary Figure S5. Three-dimensional confocal images of (a) control biofilm; (b) control biofilm cross-section. (c) Two-dimensional confocal images of control biofilm. The control biofilm was observed under 40X objective, and scanning 25 layers with 0.5 µm per step. The total biofilm thickness was around 12.5 µm.

Supplementary Figure S6. (a) Three-dimensional; and (b) two-dimensional confocal images of biofilm after contact with 100 ppm CTAB for 15 minutes; (c) the two-dimensional confocal images of live cells; and (d) the two-dimensional images of dead cells after treatment with 100 ppm CTAB for 15 minutes.

Supplementary Figure S7. Transmission Mössbauer spectra of the 11 nm MNPs (a) before and (b) after contact with MRSA biofilms for 15 min. (c) Difference plot of normalized spectra before and after contact with MRSA. Results are consistent with the biodegradation study of Yurenya et al. [S1]

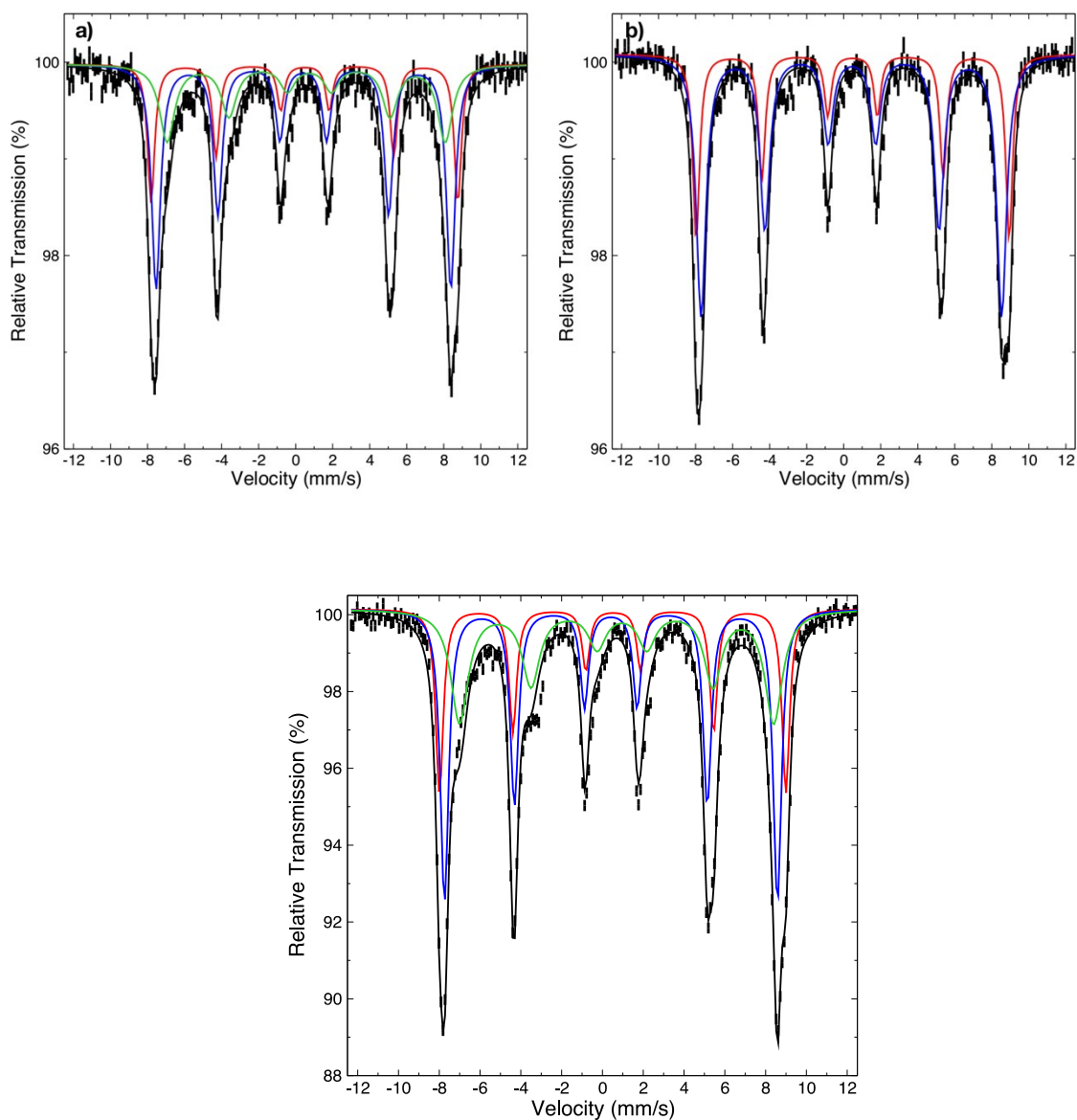
Supplementary Table S1. Mössbauer spectra fit results.

Supplementary Table S2. Antibacterial efficacy of 8 nm and 11 nm MNPs against MRSA (ATCC 33592) after 15 minutes of contact time.

Supplementary Table S3. Bacteria in the treatment and washing solution after treating MRSA biofilms with 8 nm and 11 nm MNPs according to different protocols.

Supplementary Table S4. Results of the treatment and washing solution from control biofilms after treated under the listed conditions.

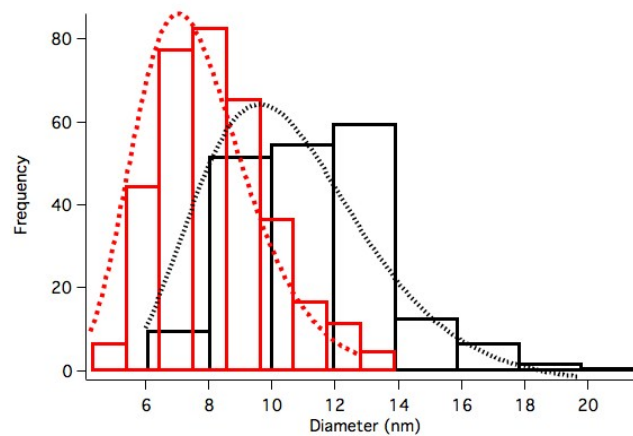
Supplementary Table S5. Mössbauer spectra fit results for 11 nm MNPs before and after contact with MRSA biofilms for 15 min.



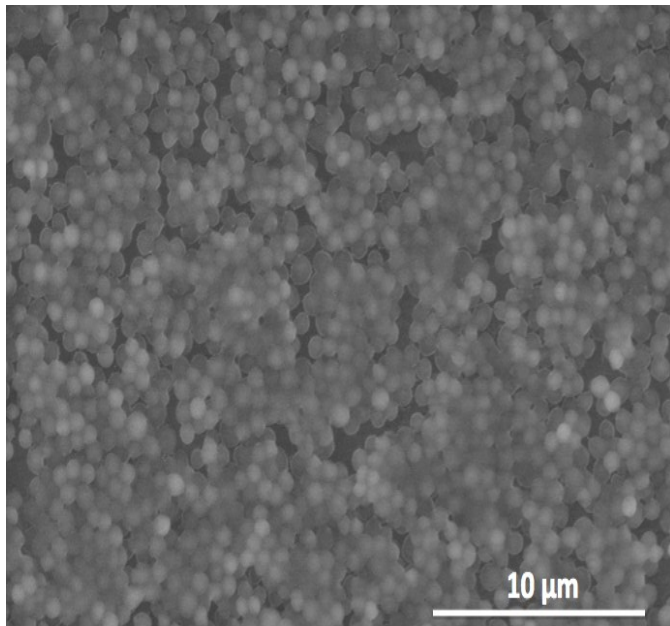
Supplementary Figure S1. Transmission Mössbauer spectra of the a) 8, b) 11 and c) 70 nm Fe_3O_4 nanoparticles. The solid lines are fits described in the text.

Supplementary Table S1. Mössbauer spectra fit results. Fitted linewidth, $\Gamma=0.24\pm 0.03$ mm/s, reflects the intrinsic chemical disorder due to finite size effects. Spectral component C is due to surface ions that suffer broken coordination and a lower hyperfine field, while A is the tetrahedral and B1 and B2 the octahedral components.

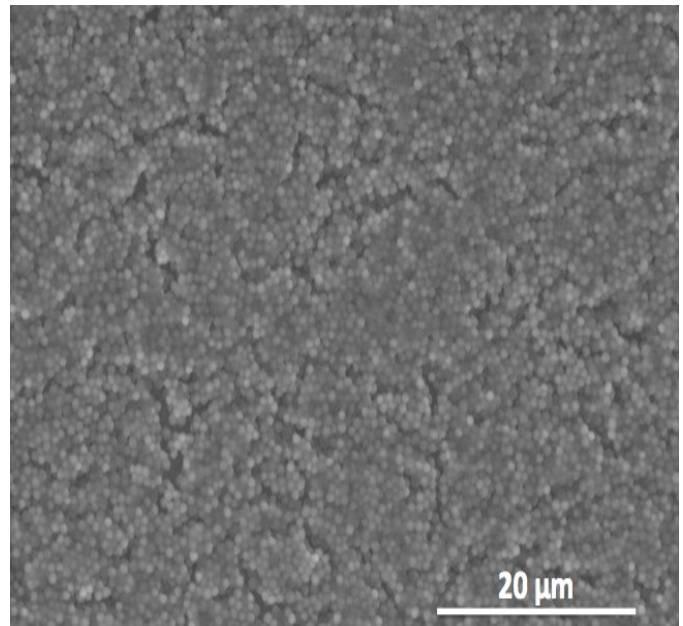
Sample	Component	Isomer Shift (mm/s)	Quadrupole Splitting (mm/s)	Hyperfine Field (T)	Area (%)
8 nm	A	0.49 ± 0.01	0	51.5 ± 0.1	24 ± 5
	B1+B2	0.416 ± 0.009	0	49.5 ± 0.1	48 ± 3
	C	0.66 ± 0.03	-0.18 ± 0.05	46.7 ± 0.3	28 ± 2
11 nm	A	0.484 ± 0.007	0	52.55 ± 0.08	33 ± 3
	B1+B2	0.432 ± 0.006	-0.03 ± 0.01	50.46 ± 0.09	67 ± 4
70 nm	A	0.517 ± 0.009	-0.03 ± 0.02	52.76 ± 0.08	42 ± 3
	B1	0.415 ± 0.006	0	50.72 ± 0.05	34 ± 5
	B2	0.83 ± 0.02	-0.26 ± 0.04	47.8 ± 0.2	24 ± 6



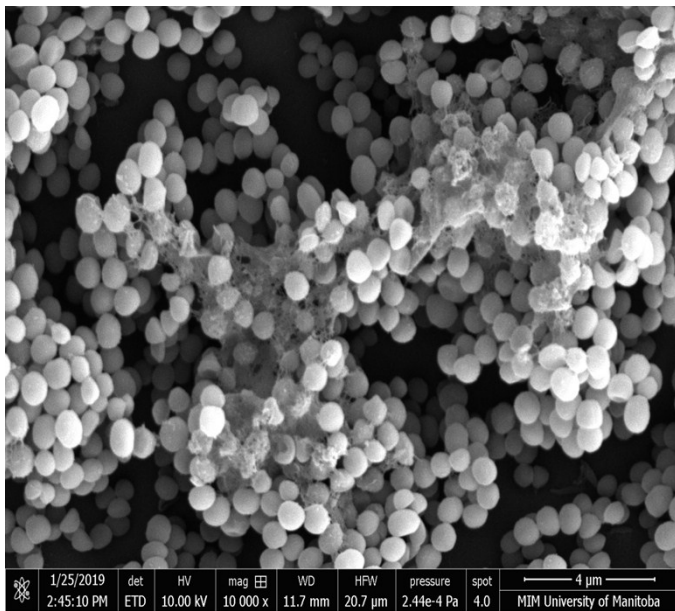
Supplementary Figure S2. Overlaid size distributions of the 8 (red, dashed line with square caps) and 11 nm (black, dashed line with flat caps) MNPs.



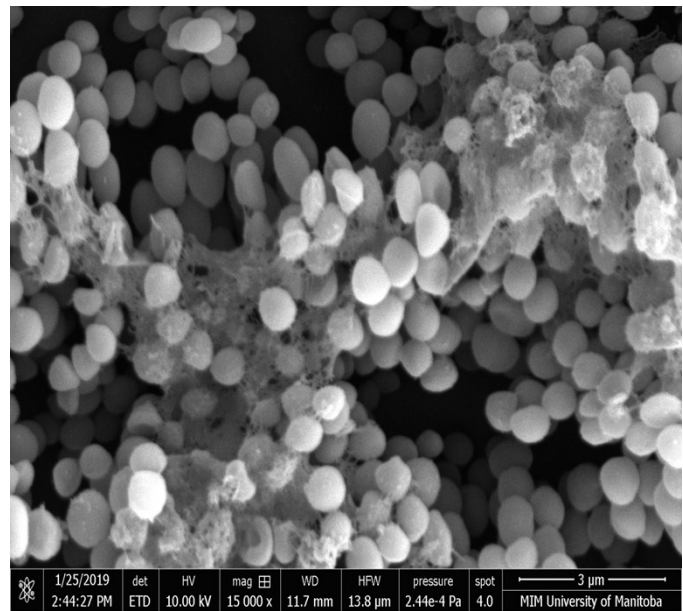
(a)



(b)

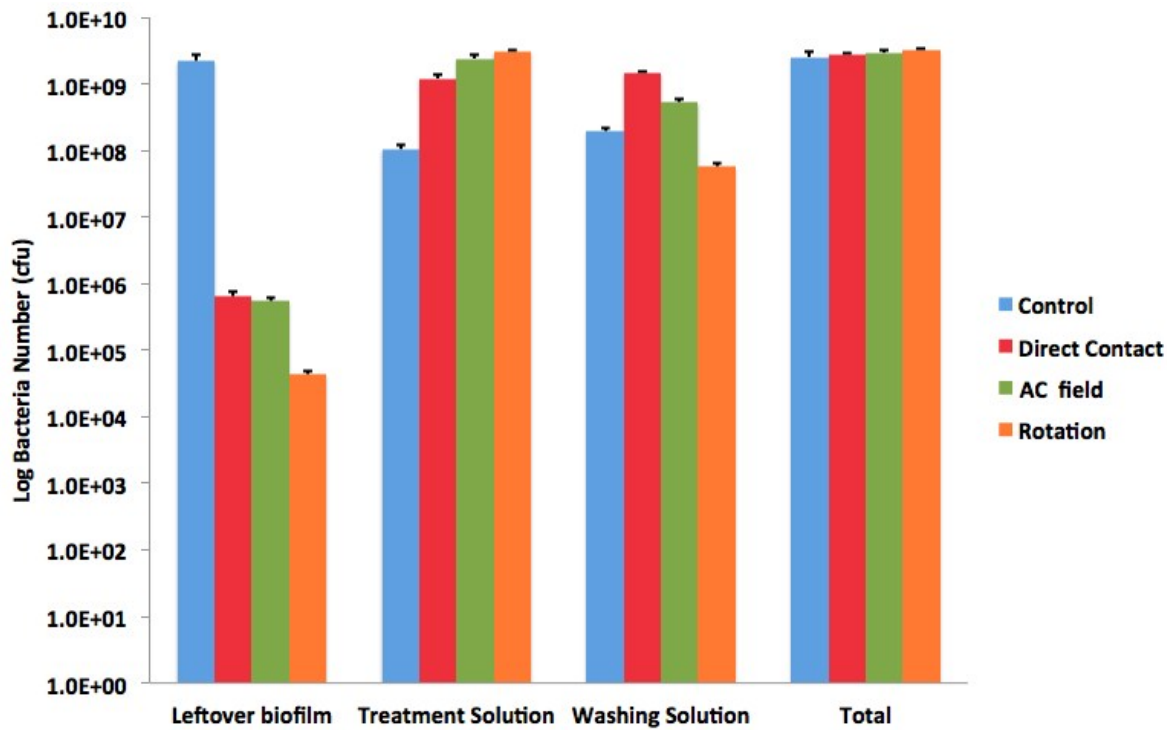


(c)



(d)

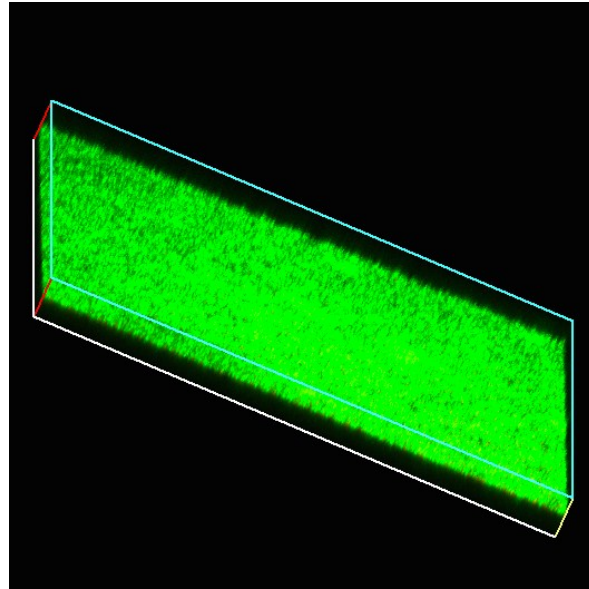
Supplementary Figure S3. (a-b) The ESEM images and (c-d) the SEM images of a control MRSA biofilm.



Supplementary Figure S4. Graph of quantified results of anti-biofilm test for 11 nm MNPs: bacterial numbers of leftover biofilm, treatment and washing solutions and the total bacteria number include bacteria in the remaining biofilm, in the treatment and washing solutions.

Supplementary Table S2. Antibacterial efficacy of 8 nm and 11 nm MNPs against MRSA (ATCC 33592) after 15 minutes of contact time.

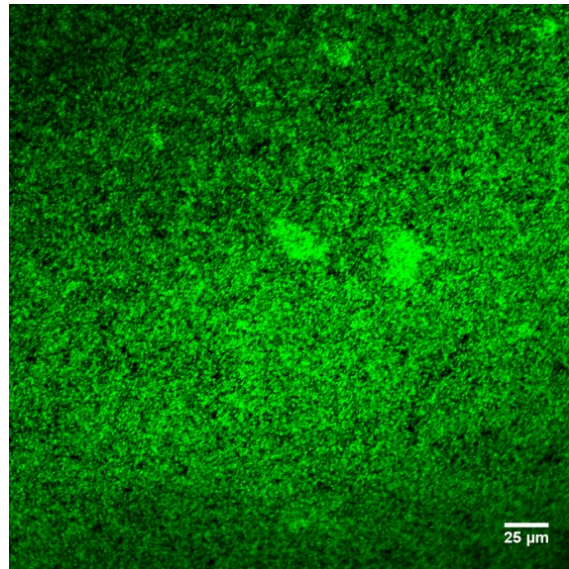
Sample	Condition	Bacterial Concentration (cfu mL⁻¹)
Control		1.1 ± 0.4 x 10 ⁹
Positive control (100 ppm CTAB)		2.4 ± 0.5 x 10 ⁸
8 nm MNPs	Direct contact	1.5 ± 0.2 x 10 ⁹
	AC field	1.2 ± 0.3 x 10 ⁹
	DC Rotation field	1.4 ± 0.3 x 10 ⁹
11 nm MNPs	Direct contact	9.5 ± 2.2 x 10 ⁸
	AC field	8.4 ± 2.5 x 10 ⁸
	DC Rotation field	1.7 ± 0.3 x 10 ⁹



(a)

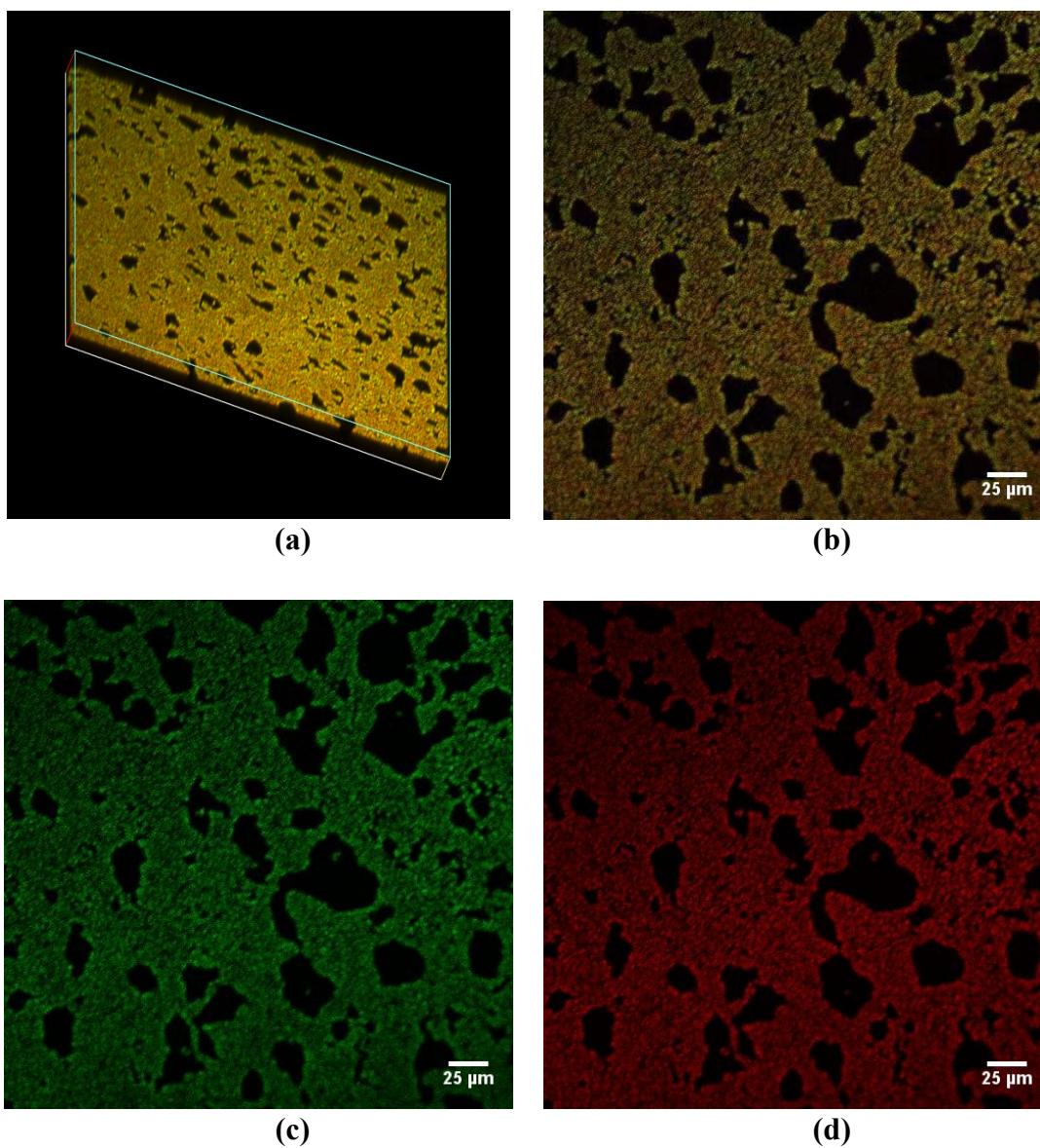


(b)



(c)

Supplementary Figure S5. Three-dimensional confocal images of (a) control biofilm; (b) control biofilm cross-section. (c) Two-dimensional confocal images of control biofilm. The control biofilm was observed under 40X objective, and scanning 25 layers with 0.5 μm per step. The total biofilm thickness was around 12.5 μm.



Supplementary Figure S6. (a) Three-dimensional; and (b) two-dimensional confocal images of biofilm after contact with 100 ppm CTAB for 15 minutes; (c) the two-dimensional confocal images of live cells; and (d) the two-dimensional images of dead cells after treatment with 100 ppm CTAB for 15 minutes.

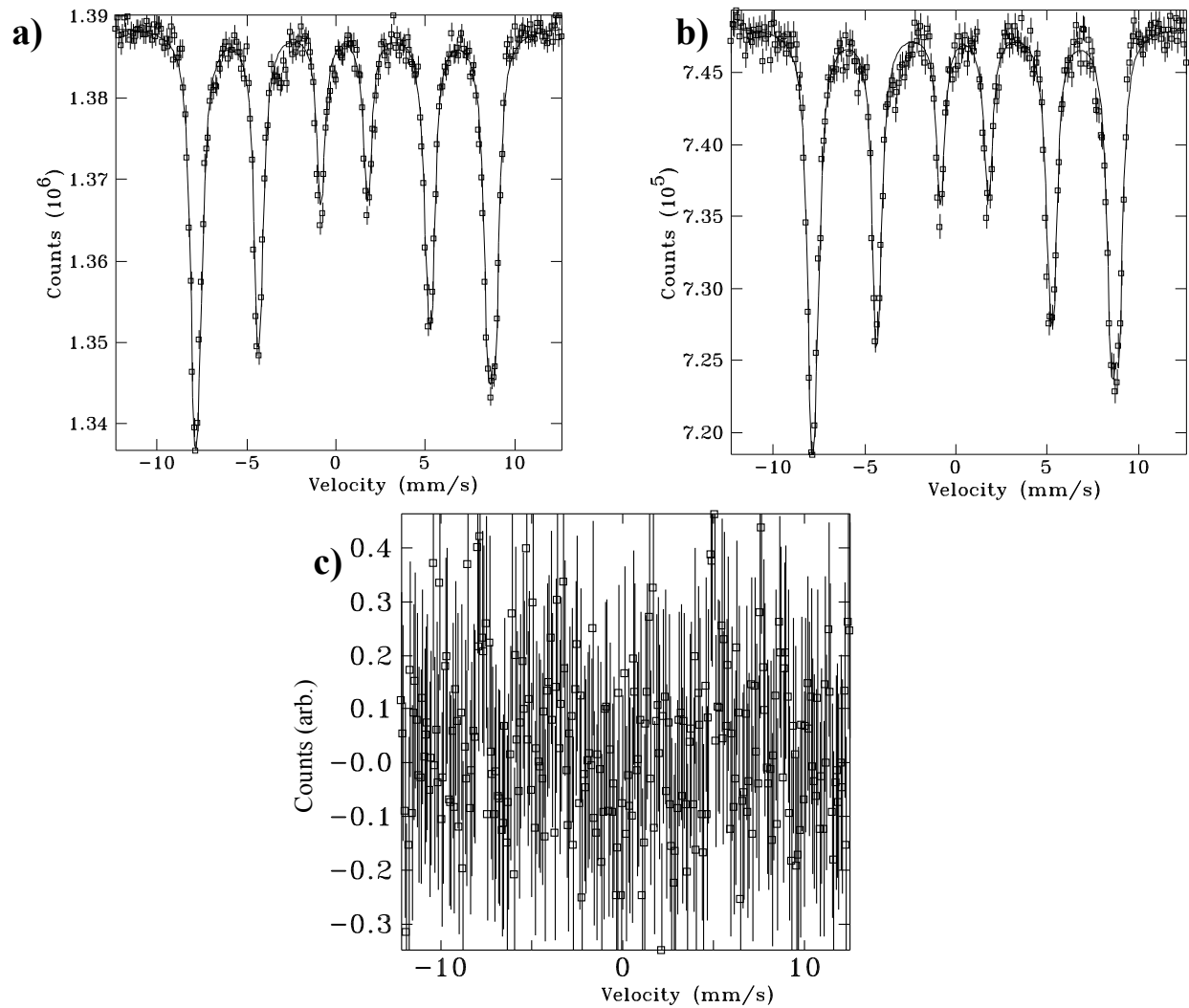
Note: These CLSM images were stained with high concentration of dyes (3 μ L of Syto 9 and 3 μ L of propidium iodide).

Supplementary Table S3. Bacteria in the treatment and washing solution after treating MRSA biofilms with 8 nm and 11 nm MNPs according to different protocols.

Samples	Conditions	Remaining biofilm (cfu)	Treatment sol'n (10⁸cfu)	Washing sol'n (10⁸cfu)	Bacterial number (T+W, 10⁸cfu)	Total (10⁹cfu)
Control		2.2 ± 0.4 x 10 ⁹	1.1 ± 0.2	2.0 ± 0.2	3.0 ± 0.1	2.5 ± 0.5
8nm MNPs	Direct contact	8.8 ± 0.3 x 10 ⁵	4.1 ± 0.3	19 ± 1	23 ± 1	2.3 ± 0.1
	AC field	7.3 ± 0.1 x 10 ⁵	17 ± 0.8	13 ± 2	30 ± 3	3.0 ± 0.2
	DC Rotation field	2.2 ± 0.2 x 10 ⁵	31 ± 4	60 ± 10	31 ± 4	3.1 ± 0.4
11nm MNPs	Direct contact	6.4 ± 1.1 x 10 ⁵	12 ± 2	15 ± 6	27 ± 2	2.7 ± 0.2
	AC field	5.4 ± 0.7 x 10 ⁵	24 ± 3	5.4 ± 0.7	30 ± 2	3.0 ± 0.2
	DC Rotation field	4.3 ± 0.5 x 10 ⁴	31 ± 2	0.6 ± 0.1	32 ± 2	3.2 ± 0.2

Supplementary Table S4. Results of the treatment and washing solution from control biofilms after treated under the listed conditions.

Sample	Remaining biofilm (cfu)	Treatment sol'n (cfu)	Washing sol'n (cfu)
RT (23 °C)	$2.1 \pm 0.2 \times 10^9$	$1.4 \pm 0.3 \times 10^8$	$6.2 \pm 0.9 \times 10^8$
24 °C	$1.8 \pm 0.4 \times 10^9$	$1.6 \pm 0.2 \times 10^8$	$6.1 \pm 1.0 \times 10^8$
30°C	$2.0 \pm 0.2 \times 10^9$	$1.6 \pm 0.2 \times 10^8$	$6.3 \pm 0.4 \times 10^8$
35°C	$2.0 \pm 0.3 \times 10^9$	$1.5 \pm 0.2 \times 10^8$	$5.9 \pm 0.8 \times 10^8$



Supplementary Figure S7. Transmission Mössbauer spectra of the 11 nm MNPs (a) before and (b) after contact with MRSA biofilms for 15 min. (c) Difference plot of normalized spectra before and after contact with MRSA. Results are consistent with the biodegradation study of Yurenya et al. [S1]

Supplementary Table S5. Mössbauer spectra fit results for 11 nm MNPs before and after contact with MRSA biofilms for 15 min.

Sample	Component	Isomer Shift (mm/s)	Quadrupole Splitting (mm/s)	Hyperfine Field (T)	Area (%)
Before contact	A	0.484 ± 0.007	0.01 ± 0.01	52.55 ± 0.08	33 ± 3
	B1+B2	0.432 ± 0.006	-0.03 ± 0.01	50.46 ± 0.09	67 ± 4
After contact	A	0.484 ± 0.009	0.01 ± 0.02	52.53 ± 0.09	35 ± 4
	B1+B2	0.432 ± 0.006	-0.03 ± 0.04	50.5 ± 0.1	65 ± 5

References

S1 A. Yurenya, A. Nikitin, A. Garanina, R. Gabbasov, M. Polikarpov, V. Cherepanov, M. Chuev, A. Majouga and V. Panchenko, *J. Magn. Magn. Mater.*, 2019, **474**, 337.